
Yoeh, Seang Shen and Yang, Tao and Tarisciotti, Luca and Hill, Christopher Ian and Bozhko, Serhiy (2016) More electric aircraft starter-generator system with utilization of hybrid modulated model predictive control. In: International Conference on Electrical Systems for Aircraft, Railway, Ship Propulsion and Road Vehicles and the International Transportation Electrification Conference (ESARS ITEC 2016), 2-4 Nov 2016, Toulouse, France.

# More Electric Aircraft Starter-Generator System with Utilization of Hybrid Modulated Model Predictive Control

Seang Shen Yeoh, Tao Yang, Luca Tarisciotti, Christopher Ian Hill, Serhiy Bozhko, Pericle Zanchetta
Department of Electrical and Electronic Engineering
University of Nottingham
Nottingham, United Kingdom
seang.yeoh@nottingham.ac.uk

***Abstract*—The current trend for future aircraft is the adoption of the More Electric Aircraft (MEA) concept. The electrical based starter-generator (S/G) system is one of the core ideas from the MEA concept. The PI based control scheme has been investigated in various papers for the permanent magnet based S/G system. Different control schemes are to be considered to improve the control performance of the S/G system. A type of non-linear control called Model Predictive Control (MPC) is considered for its capability to accomplish fast dynamic control performance. The Modulated Model Predictive Control (variant of MPC with an intrinsic modulator) was presented that showed considerably better control performance than the standard MPC. A control scheme is presented in this paper that utilises PI controllers for the outer loop and Modulated Model Predictive Control for the inner loop that covers operation for both starter and generator modes. Simulation analyses are carried out to compare between the proposed control and a full cascaded PI control scheme. The proposed control is also subjected to parameter variation tests for performance evaluation.**

***Keywords—model predictive control; starter generator; more electric aircraft***

## I. INTRODUCTION

The pressing environmental issues and increasing price of fossil fuels have been the drive to improve the weight and efficiency of aircraft. The More Electric Aircraft (MEA) concept is inline with this drive in addition to improving reliability, complexity, and costs [1, 2]. With the breakthrough of power electronics, it is possible to implement the starter-generator (S/G) scheme which is one of the core ideas of the MEA. An electrical machine can be used as a starter for the aircraft engine and function as a generator when the engine is self-sustained. The control design aspects has been reported for the MEA S/G system with a permanent magnet machine (PMM) in [3] and [4]. The designed controllers was implemented reasonably, however other control strategies should be considered to improve the control performance.

MPC has been considered as a solution for the control of power converters due to its fast dynamic performance, multivariable control, ease of constraint implementation and absence of signal modulation schemes. It can also adopted for non-minimum phase systems and handling non-linear dynamics [5, 6].

There are disadvantages of using MPC as well. Obviously since MPC is a model based control strategy, its performance largely depends on the accuracy of the model. Furthermore, the lack of a modulation scheme results in a switching state applied across the whole switching period. It may therefore result in larger ripples in controlled variables with slow switching frequencies. Large ripples in current and voltage outputs from power converters have high harmonic content and hence have lower output power quality.

The use of MPC within drive systems has been covered in [5, 7-10]. Preindl implemented MPC for torque control of a PMM drive system [7]. Similar work was also done by Bolognani in [9]. The paper highlighted the use of MPC as a multivariable controller rather than being part of the conventional cascade control structure.

A recent variant of the MPC method was introduced with an intrinsic SVM scheme called Modulated Model Predictive Control ($M^2PC$) with the aim of improving the performance of traditional MPC in terms of power quality. This method was proposed by Tarisciotti and studies have been performed in [11-15]. The aim of this method is to improve the output power quality of the system while maintaining the advantages of MPC with an intrinsic modulator. SVM was selected as the intrinsic modulator due to is efficient use of selected voltage vectors for finite switching power systems [12]. This resulted in less total harmonic distortion and switching losses from the output waveforms. The advantage offered by $M^2PC$ may be important in meeting power quality and voltage regulation standards such as MIL-STD-704F in aircraft power systems. $M^2PC$ has been investigated on IM based drive system with matrix converter [16]. In [15], $M^2PC$ has been used in a hybrid configuration with PI controllers for control of permanent magnet generator system.

In this paper, $M^2PC$ will be investigated as a control strategy for the inner current loop of the S/G power system. The outer loop will utilise PI based controllers. Together this will therefore form a hybrid control scheme. The hybrid control scheme will also be compared with the full PI control scheme done in [4]. The control scheme will be tested for both starter and generator modes at their respective operating conditions. Finally, system parameter variation will be conducted to determine the robustness of the hybrid control scheme.

The following is the structure of the paper; Section II defines the investigated electrical power system and Section III describes the control structure used. Section IV shows the simulation results to confirm the control scheme performance and the paper is concluded in the final section.

## II. Power System Model

The S/G system studied in this paper is shown in Fig. 1. $i_{abc}$ is the three phase currents, $\omega_r$ is the rotor speed, and $C$ is the DC link capacitor. $i_{dc}$ and $E_{dc}$ are the DC link current and voltage respectively. A surface mounted PMM is joined to a two level Active Front-End (AFE) rectifier. The PMM drives the aircraft engine using electrical power from the grounds or auxilliary power supply to its start-up speed (about 10krpm) in starter mode. After that process, the engine proceeds to accelerate to higher speeds using its main power source which is jet fuel. At high speeds, the PMM functions as a generator to deliver electrical power to the main DC bus via the AFE. In generator mode, the aircraft engine is controlled externally and is assumed as an ideal speed source for the S/G system. The control scheme for this S/G system will be described in Section III.

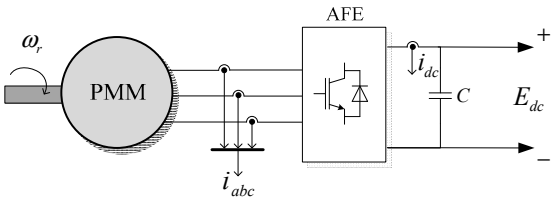


Fig. 1. S/G power system in study.

For the investigated S/G system, the model equations for MPC are mainly based on the PMM electrical equations (1) and (2):

$$v_d = R_s i_d(t) + L_d \frac{di_d(t)}{dt} - L_q \omega_e(t) i_q(t) \quad (1)$$

$$v_q = R_s i_q(t) + L_q \frac{di_q(t)}{dt} + \left(L_d i_d(t) + \psi_m\right)\omega_e(t) \quad (2)$$

where $R_s$ is the stator resistance, $\psi_m$ is the mutual flux of the machine, and $\omega_e$ is the electrical speed. $v_{d,q}$ and $i_{d,q}$ are the AC voltages and currents of the PMM in $dq$ frame. $L_{d,q}$ are the PMM inductances in $dq$ frame. The derivative terms within these equations are discretised using the forward Euler method. It is assumed that the state variables stay constant during the sampling period, $T_s$.

$$\frac{di(t)}{dt} \approx \frac{i(k+1) - i(k)}{T_s} \quad (3)$$

The discrete model for the PMM can therefore be derived as:

$$v_d(k) = R_s i_d(k) + \frac{L_d\left(i_d(k+1) - i_d(k)\right)}{T_s} - L_q \omega_e(k) i_q(k) \quad (4)$$

$$v_q(k) = R_s i_q(k) + \frac{L_q\left(i_q(k+1) - i_q(k)\right)}{T_s} + L_d \omega_e(k) i_d(k) + \psi_m \omega_e(k) \quad (5)$$

$v_{d,q}$ can be related to the switching states of the AFE in the $dq$ frame, $S_{d,q}$, and $E_{dc}$, by the following equation if the impedance of the transmission line between the AFE and PMM is neglected:

$$v_{d,q} = E_{dc} k_{dq} S_{d,q} \quad (6)$$

$k_{dq}$ represents the $dq$ transformation matrix where three-phase variables can be transformed to $dq$ frame:

$$\begin{bmatrix} x_d(k) \\ x_q(k) \end{bmatrix} = k_{dq} \begin{bmatrix} x_a(k) \\ x_b(k) \\ x_c(k) \end{bmatrix} \quad (7)$$

$$k_{dq} = \frac{2}{3} \begin{bmatrix} \cos(\theta(k)) & \cos\left(\theta(k) - \frac{2\pi}{3}\right) & \cos\left(\theta(k) + \frac{2\pi}{3}\right) \\ -\sin(\theta(k)) & -\sin\left(\theta(k) - \frac{2\pi}{3}\right) & -\sin\left(\theta(k) + \frac{2\pi}{3}\right) \end{bmatrix} \quad (8)$$

## III. Control Approach

The advantage of MPC is its capability to predict future states over a fixed time horizon based on the control inputs and measured present states. For a power converter, this data is optimised within a cost minimisation function that decides the converter switching states for the next sampling period. The most suitable switching state is then selected and sent to the converter. Since a converter has a finite number of switching states, the optimisation stage and the time it takes can be reduced. The procedure of prediction and cost minimisation recurs for every sampling period [5, 6]. The flow diagram summarising the procedure can be seen in Fig. 2.

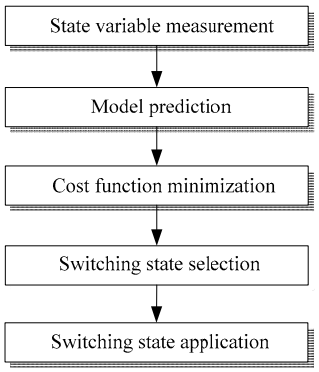


Fig. 2. Generalised MPC flow diagram.

The control of this S/G system is centred on field oriented vector control where $i_d$ and $i_q$ are regulated to produce appropriate voltage vectors. Fig. 4 shows the proposed hybrid PI-M$^2$PC. Variables with superscript * denote their respective reference values. $|V|$ is the AC magnitude voltage, $v_1$ and $v_2$ are the two active voltage vectors while $v_{01}$ and $v_{02}$ are the two zero voltage vectors. $i_{qlim}$ is the limit for the dynamic limiter that is derived from the maximum stator current, $i_m$ and $i_d$.

The control scheme for the S/G system can be divided into two parts; inner and outer loop. The choice of outer loop controller variables are as follows: the speed controller, $W_s$, is used during starter mode and switches to the DC link voltage controller, $W_{idc}$, when operating in generator mode. Droop control is employed together with $W_{idc}$ to enable parallel source operation if required. The flux weakening controller, $W_{fw}$, is always connected to ensure control operation of the S/G system throughout the speed range. PI based controllers will be used for the outer loop.

The inner loops control $i_d$ and $i_q$ using MPC as explained earlier in this section. Due to a computational delay that exists in the practical system, the control output calculated at time instant $k$ can only be implemented at time instant $k+1$. This delay can be circumvented by calculating values two steps ahead. Equations (4) and (5) can be re-formed for two step prediction to give:

$$i_d(k+2) = -\frac{R_s T_s i_d(k+1)}{L_d} + i_d(k+1) + \frac{\omega_e(k+1) T_s L_q i_q(k+1)}{L_d} + \frac{T_s v_d(k+1)}{L_d} \tag{9}$$

$$i_q(k+2) = \left[ -\frac{R_s T_s i_q(k+1)}{L_q} + i_q(k+1) - \frac{\omega_e(k+1) T_s L_d i_d(k+1)}{L_q} + \frac{T_s v_q(k+1)}{L_q} - \frac{\psi_m \omega_e(k+1) T_s}{L_q} \right] \tag{10}$$

Now that the model equations are established, the cost function, $g_{MPC}$, can be defined as:

$$g_{MPC} = \left| i_d^* - i_d^i(k+2) \right| + \left| i_q^* - i_q^i(k+2) \right| \tag{11}$$

The currents are predicted considering all possible switching states. In this study a two-level converter is utilised and so as such eight switching states are possible. The switching state for $k + 2$ that gives the smallest cost function is selected and applied at the next sampling period.

### A. Modulated Model Predictive Control

In general, M$^2$PC has similar prediction pattern to the MPC except with the addition of modulation stage for SVM. Since SVM is used for the modulation scheme, two active voltage vectors ($v_1$, $v_2$) are required for M$^2$PC operation. The two active vectors are designated from all the possible vector pairs by means of a modified cost function that takes into account the voltage, current, and duty cycle predictions. The duty cycles, $d$ determine the appropriate time ratio for the four selected vectors ($v_1$, $v_2$, $v_{01}$, $v_{02}$) within each sampling period, as shown in Fig. 3. Finally, the appropriate switching states are to be applied over a series of modulation steps, $m_s$.

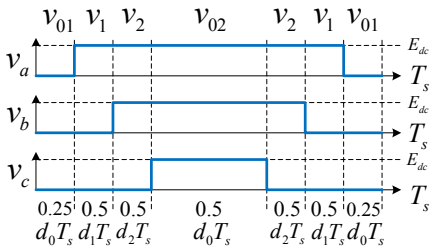


Fig. 3. M$^2$PC typical switching pattern [11].

The two active vectors for SVM are to be predicted based on (9) and (10), and these will be used to determine $i^i_{d,q}(k+2)$ and $i^j_{d,q}(k+2)$. The variables with superscript $i$ and $j$ use switch vectors in the order of [1,2,3,4,5,6] and [2,3,4,5,6,1] respectively. (4) and (5) are utilised to calculate the zero vector currents, $i^0_{d,q}(k+2)$ when $v_{d,q} = 0$. Equation (6) can then be re-arranged to give:

$$v_d^* = E_{dc}\left[ d_1 S_d^i + d_2 S_d^j \right] \tag{12}$$

$$v_q^* = E_{dc}\left[ d_1 S_q^i + d_2 S_q^j \right] \tag{13}$$

where $d_1$ and $d_2$ are the duty cycles for $v_1$ and $v_2$ respectively. The type of M$^2$PC used in this study is based on the dead beat control variation [11]; hence the voltage references for the model also has to be predicted. $v_{d,q}^*$ can then be predicted to be equal to the voltage change across the inductances:

$$v_d^*(k+1) = \frac{\Delta i_d(k+1) L_d}{T_s} \tag{14}$$

$$v_q^*(k+1) = \frac{\Delta i_q(k+1) L_q}{T_s} \tag{15}$$

where

$$\Delta i_d(k+1) = i_d^0(k+1) - i_d^* \tag{16}$$

$$\Delta i_q(k+1) = i_q^0(k+1) - i_q^* \tag{17}$$

The zero vector duty cycle, $d_0$, can then be determined with:

$$d_0 = 1 - d_1 - d_2 \tag{18}$$

M$^2$PC requires two cost functions for the two active vectors:

$$g_{M^2PC1} = \left| i_d^* - i_d^i(k+2) \right| + \left| i_q^* - i_q^i(k+2) \right| \tag{19}$$

$$g_{M^2PC2} = \left| i_d^* - i_d^j(k+2) \right| + \left| i_q^* - i_q^j(k+2) \right| \tag{20}$$

Together with $d_1$ and $d_2$, the overall cost function, $g_{M2PC}$, is the sum of the two cost functions:

$$g_{M^2PC} = d_1 g_{M^2PC1} + d_2 g_{M^2PC2} \tag{21}$$

The switching states of $S^i_{d,q}$ and $S^j_{d,q}$ that generates the smallest $g$ will therefore be applied in the three-phase frame accodring to the duty cycles of $d_1$ and $d_2$ using the modulation scheme.

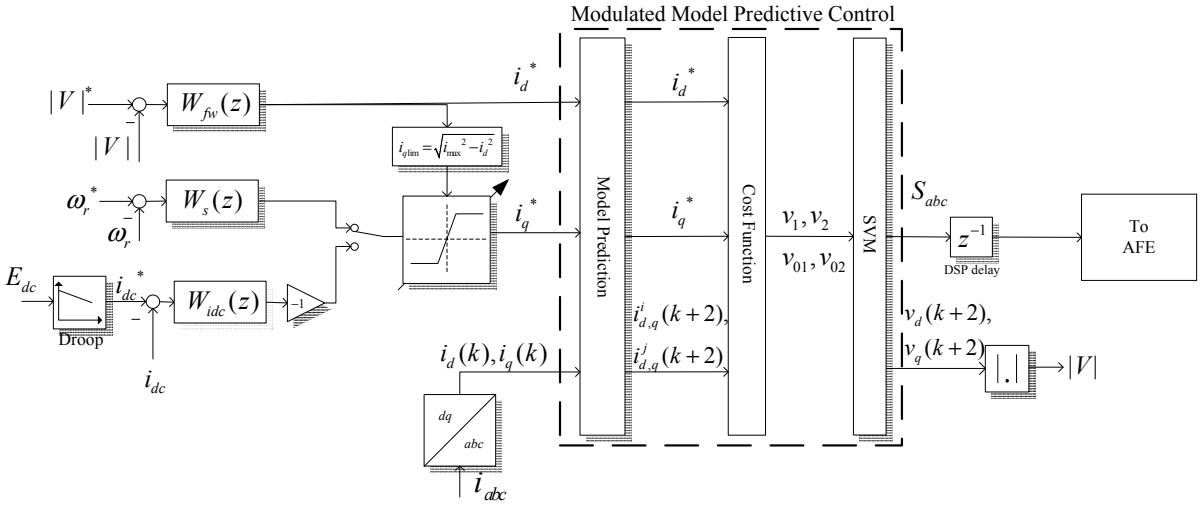


Fig. 4. Hybrid PI – M²PC scheme.

### B. Angle Compensation

For high speed drive systems, [10] mentioned that the electrical angle, $\theta$, has to be compensated. The reason is that $\theta$ is proportional to the machine rotor position, $\theta_r$, and therefore there would be a difference between the actual and predicted rotor position depending on the operating speed. In order to reduce this error, $\theta_r$ has to be compensated 1.5 sample periods ahead in order to obtain the mean rotor position after one sample delay. This can be represented by:

$$\theta(k+1) = 1.5\, p\omega_r(k) T_s + \theta(k) \qquad (22)$$

## IV. Results and Analysis

After having derived the control structure, it is tested with a non-linear Matlab®/Simulink® model of the S/G system. The system parameters used are given in Table 1. The modulation step is the ratio between the PWM carrier signal frequency and sampling frequency. The modulation frequency is the rate at which the control signals are sampled. The full PI control scheme designed in [4] was used as a benchmark model.

Table 1. System parameters.

| Parameter | Value |
|---|---|
| Stator resistance, $R_s$ | $1.058m\Omega$ |
| Stator inductance in rotating frame, $L_d$ = $L_q$ | $99\mu H$ |
| Pole pairs, $p$ | 3 |
| Magnet flux-linkage, $\psi_m$ | $0.03644Vs$ |
| Rated power, $P_{rated}$ | $45kW$ |
| Combined machine and engine inertia, $J$ | $0.103kgms^2$ |
| DC bus capacitance, $C$ | $1.2mF$ |
| Sampling period, $T_s$ | $62.5\mu s$ |
| Modulation period, $T_m$ | $625ns$ |
| Modulation step, $m_s = T_m/T_s$ | 100 |

### A. S/G Operation with Hybrid Control

Fig. 5 shows the responses of the key state variables during starter mode. The speed reference is set at 20krpm. FW was operational when $|V|$ reached its reference value of 155V by $i_d$ injection into the machine, as clearly seen in the simulation results from $t \sim 1.5$s.

Once the S/G system reached steady state, a load, $T_L$, of 10Nm was applied at $t$ = 5s. The controlled variables $|V|$ and $\omega_r$, which use outer loop PI based controllers, have no steady state error after the $T_L$ was applied due to the integral terms within their respective regulators. Using the hybrid PI-M²PC scheme, significant $dq$ current ripple reduction was observed throughout the simulation due to the use of M²PC as part of the control structure.

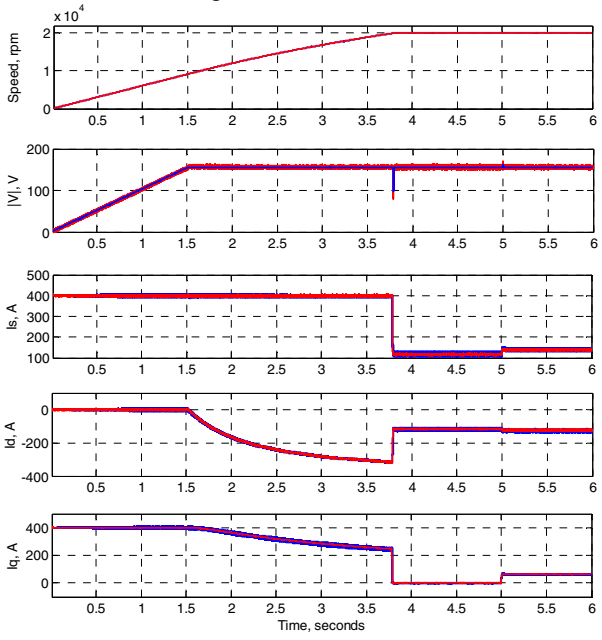


Fig. 5. Time domain simulation in starter mode up to 20krpm between the full PI (blue) and hybrid PI-M²PC scheme (red).

Fig. 6 shows the key state variable responses using the two control schemes in generator mode. During this

simulation the DC bus accepted load demands of 50A, 100A, 130A, and 170A in 0.03s intervals. Both of the control schemes were able to function with the subjected electrical loads at 32krpm. Significant reduction in the current and $|V|$ ripple was observed when using the hybrid PI-M$^2$PC. When the electrical loads were applied, there was almost zero difference in the steady state ripple for $E_{dc}$. It can be seen that there was a more underdamped response for all of the state variables when using the hybrid PI-M$^2$PC scheme.

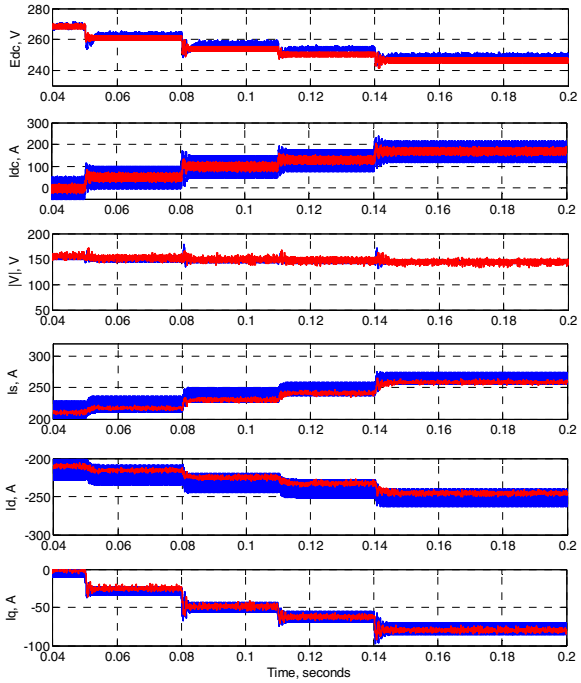


Fig. 6. Time domain simulation in generator mode operating at 32krpm between the full PI (blue) and hybrid PI-M$^2$PC scheme (red).

## B. Parameter Variation

For model based controllers such as MPC, it is important to assess the robustness of the technique towards parameter changes in the power system, especially if there are no parameter observer algorithms to adapt to the changes. Therefore, in order to test the robustness of the hybrid control scheme, parameter variation was introduced within the simulation model. Parameters that could change in actual drive systems due to operating temperature or other factors such as $R_s$, $L_{d,q}$, $\psi_m$, and $C$ were assessed. Any significant changes in the state variables could then be observed through the $dq$ currents along with the parameter difference from its nominal value.

Fig. 7 shows the $i_q$ response when $R_s$ was altered by 5, 10, 40, 70, and 100 times its nominal value (1.058m$\Omega$). The figure also shows the responses when subjected to a step in electrical load of 10kW at $t$ = 0.08s. This was included in order to determine any differences before and after load impact. It can be seen that there was a difference in steady state values that are increasing (in the negative direction) as $i_q$ had to compensate for the higher $R_s$. Even at 100 times the nominal value of $R_s$, the control was still stable.

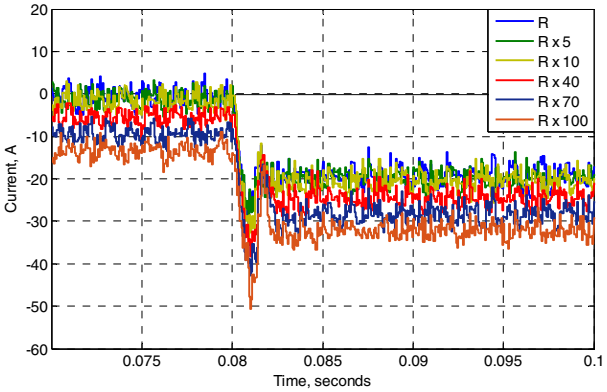


Fig. 7. $i_q$ responses with different values of $R_s$ operating at 32krpm.

Both $L_d$ and $L_q$ were reduced simultaneously in increments of 5% of their nominal value with the same load conditions as the $R_s$ variation test. Both $dq$ currents were found to be affected by the change in inductance, as can be seen in Fig. 8. Large ripples can be seen when the $dq$ inductances were at 80% of the nominal value (99µH). The variation in $L_d$ and $L_q$ affects the accuracy of the model prediction and as such causes the different steady state values of $i_d$.

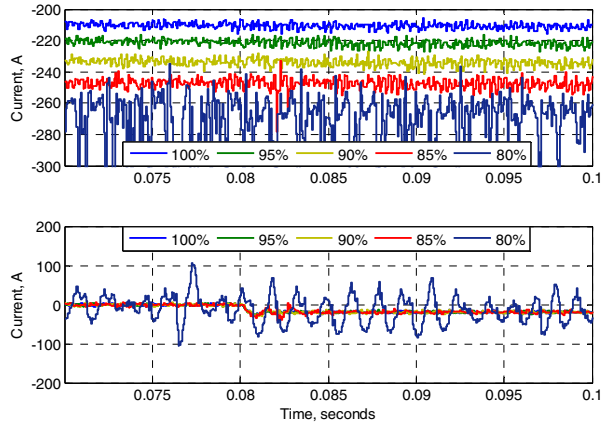


Fig. 8. $i_d$ (top) and $i_q$ (bottom) responses with different values of machine inductance operating at 32krpm.

$\psi_m$ was reduced in increments of 5% of its nominal value. Both of the $dq$ currents were observed and are shown in Fig. 9. The change of $\psi_m$ resulted in different steady state results for $i_d$ due to the decrease of back-emf. Less $i_d$ was therefore required for FW. Large ripples were observed at 80% $\psi_m$ when operating without load. After the load impact of 10kW, the large oscillations reduced and stability was restored. Fig. 10 shows $i_q$ responses to changes of $C$ when reduced by 20% increments. The reduction of $C$ mainly affected $W_{idc}$ which explains the oscillations.

Overall, the influence of $L$ and $\psi_m$ variation imposed the most significant effect to the hybrid M$^2$PC control performance. A maximum change of 20% $L$ or 25% $\psi_m$ was required before the controller became unstable. In applications where the actual system parameters can vary beyond this range, observers can be used for parameter estimation such as Luenberger observer and Kalman filter.

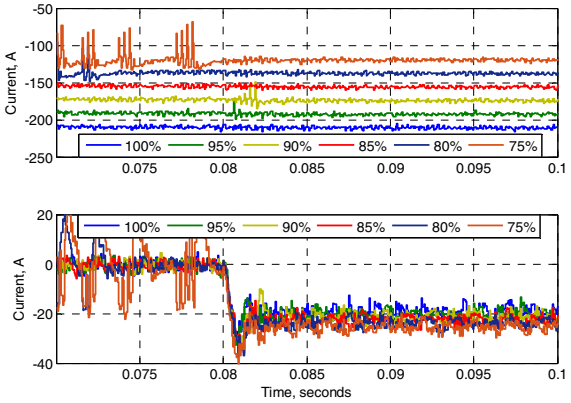


Fig. 9. $i_d$ (top) and $i_q$ (bottom) responses with different values of $\psi_m$ operating at 32krpm.

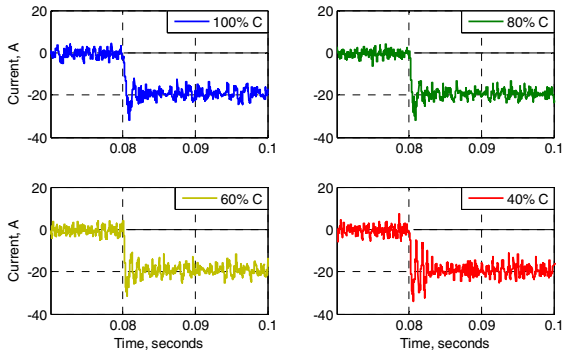


Fig. 10. $i_q$ responses with different values of $C$ operating at 32krpm.

## V. Conclusion

M$^2$PC was investigated to assess its potential for improving the control performance of the S/G system. The M$^2$PC scheme was derived and implemented for the *dq* current loop. The outer control loops were controlled using PI controllers. Angle compensation was therefore added as the model prediction was being affected by the speed of the PMM. Overall, the hybrid PI-M$^2$PC scheme was found to be capable of S/G control operation. Moreover, it showed improvements in terms of reduced current ripple when compared to the conventional full PI control scheme. Parameter variation tests showed that the hybrid control performance was most susceptible to the change of $L$ and $\psi_m$ within a variation of 20% and 25% respectively. Parameter observers are required to compensate for possible parameter variations beyond that range. Future work would include experimental verification of the hybrid control scheme and implementation of full predictive control (Speed, FW, and DC link voltage as part of predictive control variables) for the S/G system.

## Acknowledgement

The work in this paper has been funded by EU FP7 funding via the Clean Sky JTI (Systems for green Operations ITD).

## References

[1] J. A. Rosero, J. A. Ortega, E. Aldabas, and L. Romeral, "Moving towards a more electric aircraft," *Aerospace and Electronic Systems Magazine, IEEE,* vol. 22, pp. 3-9, 2007.

[2] P. Wheeler and S. Bozhko, "The More Electric Aircraft: Technology and challenges," *Electrification Magazine, IEEE,* vol. 2, pp. 6-12, 2014.

[3] S. Bozhko, Y. Seang Shen, G. Fei, and C. Hill, "Aircraft starter-generator system based on permanent-magnet machine fed by active front-end rectifier," in *Industrial Electronics Society, IECON 2014 - 40th Annual Conference of the IEEE*, 2014, pp. 2958-2964.

[4] S. S. Yeoh, F. Gao, S. Bozhko, and G. Asher, "Control design for PMM-based starter generator system for More Electric Aircraft," in *Power Electronics and Applications (EPE'14-ECCE Europe), 2014 16th European Conference on*, 2014, pp. 1-10.

[5] P. Cortes, M. P. Kazmierkowski, R. M. Kennel, D. E. Quevedo, and J. Rodriguez, "Predictive Control in Power Electronics and Drives," *Industrial Electronics, IEEE Transactions on,* vol. 55, pp. 4312-4324, 2008.

[6] J. Rodriguez, M. P. Kazmierkowski, J. R. Espinoza, P. Zanchetta, H. Abu-Rub, H. A. Young, and C. A. Rojas, "State of the Art of Finite Control Set Model Predictive Control in Power Electronics," *Industrial Informatics, IEEE Transactions on,* vol. 9, pp. 1003-1016, 2013.

[7] M. Preindl and S. Bolognani, "Model Predictive Direct Speed Control with Finite Control Set of PMSM Drive Systems," *Power Electronics, IEEE Transactions on,* vol. 28, pp. 1007-1015, 2013.

[8] M. Preindl and S. Bolognani, "Model Predictive Direct Torque Control With Finite Control Set for PMSM Drive Systems, Part 1: Maximum Torque Per Ampere Operation," *Industrial Informatics, IEEE Transactions on,* vol. 9, pp. 1912-1921, 2013.

[9] S. Bolognani, L. Peretti, and M. Zigliotto, "Design and Implementation of Model Predictive Control for Electrical Motor Drives," *Industrial Electronics, IEEE Transactions on,* vol. 56, pp. 1925-1936, 2009.

[10] M. Hyung-Tae, K. Hyun-Soo, and Y. Myung-Joong, "A discrete-time predictive current control for PMSM," *Power Electronics, IEEE Transactions on,* vol. 18, pp. 464-472, 2003.

[11] L. Tarisciotti, P. Zanchetta, A. Watson, J. Clare, M. Degano, and S. Bifaretti, "Modulated Model Predictive Control (M2PC) For A 3-Phase Active Rectifier," *Industry Applications, IEEE Transactions on,* vol. PP, pp. 1-1, 2014.

[12] L. Tarisciotti, "Model Predictive Control for Advanced Multilevel Power Converters in Smart-Grid Applications," PhD, University of Nottingham, 2014.

[13] L. Tarisciotti, P. Zanchetta, A. Watson, J. Clare, S. Bifaretti, and M. Rivera, "A new predictive control method for cascaded multilevel converters with intrinsic modulation scheme," in *Industrial Electronics Society, IECON 2013 - 39th Annual Conference of the IEEE*, 2013, pp. 5764-5769.

[14] L. Tarisciotti, P. Zanchetta, A. Watson, S. Bifaretti, and J. C. Clare, "Modulated Model Predictive Control for a Seven-Level Cascaded H-Bridge Back-to-Back Converter," *Industrial Electronics, IEEE Transactions on,* vol. 61, pp. 5375-5383, 2014.

[15] Y. Seang Shen, Y. Tao, L. Tarisciotti, S. Bozhko, and P. Zanchetta, "Hybrid modulated model predictive control for the more electric aircraft generator system," in *Electrical Systems for Aircraft, Railway, Ship Propulsion and Road Vehicles (ESARS), 2015 International Conference on*, 2015, pp. 1-6.

[16] M. Vijayagopal, L. Empringham, L. de Lillo, L. Tarisciotti, P. Zanchetta, and P. Wheeler, "Control of a direct matrix converter induction motor drive with modulated model predictive control," in *Energy Conversion Congress and Exposition (ECCE), 2015 IEEE*, 2015, pp. 4315-4321.